JACS
JOURNAL OF THE AMERICAN CHEMICAL SOCIETY

COMMUNICATION

pubs.acs.org/JACS

A Mitochondrial-Targeted Two-Photon Probe for Zinc Ion

Goutam Masanta,[†] Chang Su Lim,[§] Hyung Joong Kim,[‡] Ji Hee Han,[§] Hwan Myung Kim,*[,†,‡] and Bong Rae Cho*[,§]

[†]Molecular Science and Technology Research Center, [‡]Division of Energy Systems Research, Ajou University, Suwon 443-749, Korea
[§]Department of Chemistry, Korea University, 1-Anamdong, Seoul 136-701, Korea

Supporting Information

ABSTRACT: We report a two-photon probe (SZn-Mito) for mitochondrial zinc ions ($[Zn^{2+}]_m$). This probe shows a 7-fold enhancement of two-photon-excited fluorescence in response to Zn^{2+} with a dissociation constant (K_d^{TP}) of 3.1 ± 0.1 nM and pH insensitivity in the biologically relevant range, allowing the detection of $[Zn^{2+}]_m$ in a rat hippocampal slice at a depth of 100−200 μm without interference from other metal ions through the use of two-photon microscopy.

Zinc is the second most abundant transition-metal ion in the human body.[1] In the brain, 5−20% of the total Zn^{2+} is stored in presynaptic vesicles, and the highest intracellular free Zn^{2+} ($[Zn^{2+}]_i$) is found in the hippocampus.[2] Zn^{2+} modulates brain excitability and plays a key role in synaptic plasticity.[3] For proper brain function, maintaining $[Zn^{2+}]_i$ homeostasis is vital. Imbalance in $[Zn^{2+}]_i$ has been linked to neurological disorders such as Alzheimer's and Parkinson's diseases.[4] Recent studies suggest that mitochondria take up evoked $[Zn^{2+}]_i$ increases, thereby controlling the $[Zn^{2+}]_i$ homeostasis.[5,6] On the other hand, a strong elevation of intramitochondrial Zn^{2+} ($[Zn^{2+}]_m$) concentration can promote mitochondrial dysfunction and generation of reactive oxygen species (ROS).[5,6] To understand the physiology of Zn^{2+} in the brain, it is crucial to monitor $[Zn^{2+}]_m$ in intact brain tissues.

To detect $[Zn^{2+}]_m$ in cells, a one-photon (OP) fluorescent probe (RhodZin-3) has been developed and commercialized.[7,8] This small-molecule probe does not require transfection, as does its protein counterparts,[9,10] but it suffers from the lack of selectivity for mitochondria and/or Zn^{2+}.[8,9b,10] Moreover, use of this probe with one-photon microscopy (OPM) requires a rather short excitation wavelength (~550 nm) that limits its use in tissue imaging because of the shallow penetration depth (<100 μm), photobleaching, and cellular autofluorescence. Overcoming these problems requires a two-photon (TP) probe that can be used for detection of $[Zn^{2+}]_m$ in intact tissues through two-photon microscopy (TPM). TPM, which utilizes two photons of lower energy for the excitation, is a new technique that can visualize biological events deep inside intact tissues (>500 μm) for extended periods of time.[11,12] We therefore designed a new TP probe for $[Zn^{2+}]_m$, SZn-Mito (Scheme 1), which is derived from 6-(benzo[*d*]thiazol-2′-yl)-2-(*N*,*N*-dimethylamino)naphthalene (BTDAN) as the reporter, *N*,*N*-di-(2-picolyl)-ethylenediamine (DPEN) as the Zn^{2+} chelator, and triphenylphosphonium salt (TPP) as the mitochondrial-targeting site.[13−15] BTDAN is closely related to 6-(benzo[*d*]oxazol-2′-yl)-2-(*N*,*N*-dimethylamino)naphthalene, which has been successfully utilized in the TP probe for Ca^{2+} (BCaM);[16] DPEN is a well-known receptor for Zn^{2+},[13] and TPP is an effective mitochondrial-targeting site.[14,15] DPEN and TPP are separated as far as possible to minimize the interactions between them. Herein we report that SZn-Mito can be used for selective detection of $[Zn^{2+}]_m$ in live cells and intact tissues at >100 μm depth by TPM.

Scheme 1. Synthesis of SZn-Mito[a]

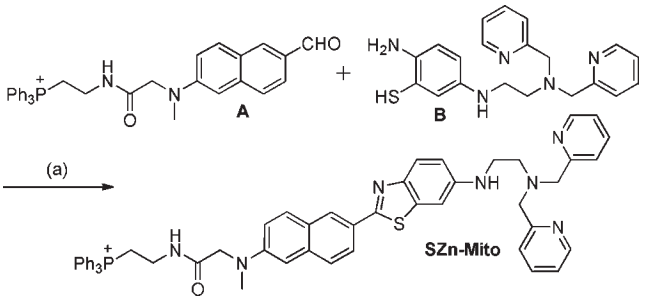

[a] Conditions (a): *p*-toluenesulfonic acid, $CHCl_3$.

The preparation of SZn-Mito is described in the Supporting Information (SI). The solubility of SZn-Mito in 3-(*N*-morpholino)propanesulfonic acid (MOPS) buffer solution (30 mM, 100 mM KCl, pH 7.2) as determined by the fluorescence method[17] is ~2 μM, which is sufficient to stain the cells (Figure S2 in the SI).

The photophysical properties of SZn-Mito were studied in MOPS buffer solution. In metal-free buffer (30 mM MOPS, 100 mM KCl, 10 mM EGTA, pH 7.2), SZn-Mito has absorption and emission maxima at 388 nm ($\varepsilon = 1.87 \times 10^4\ M^{-1}\ cm^{-1}$) and 500 nm ($\Phi = 0.15$), respectively. Both spectra showed gradual red shifts with increasing solvent polarity (Figure S1 and Table S1). The shifts were greater for the fluorescence spectrum (45 nm) than for the absorption spectrum (5 nm). Upon addition of Zn^{2+}, the fluorescence intensity increased dramatically ($\Phi = 0.92$) and exhibited a slight blue shift in both its absorption (375 nm, $\varepsilon = 2.31 \times 10^4\ M^{-1}\ cm^{-1}$) and emission maxima (493 nm) (Figure S3a,b). This outcome can be attributed to the blocking of the photoinduced electron transfer process and the decrease in the electron-donating ability of the amino group by the complexation of SZn-Mito with Zn^{2+}, of which the former appears to be predominant. A nearly identical result was observed in the TP process (Figure 1a). The fluorescence enhancement factors [FEF = $(F - F_{min})/F_{min}$] of SZn-Mito determined for the OP and TP processes were both equal to 7 in the presence of excess Zn^{2+} (Table S2).

Received: January 17, 2011
Published: March 30, 2011

dx.doi.org/10.1021/ja200444t | *J. Am. Chem. Soc.* 2011, 133, 5698–5700

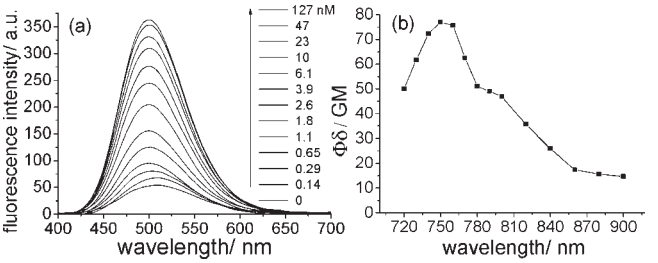

Figure 1. (a) Two-photon fluorescence spectra of 1 μM SZn-Mito in the presence of free Zn^{2+} (0−127 nM). The excitation wavelength was 760 nm. (b) Two-photon action spectrum of SZn-Mito in the presence of 47 nM free Zn^{2+}. These data were measured in 30 mM MOPS buffer (100 mM KCl, 10 mM EGTA, pH 7.2).

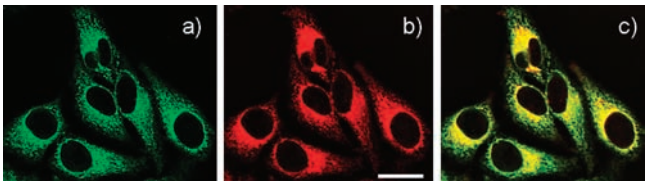

Figure 2. (a) TPM and (b) OPM images of HeLa cells colabeled with (a) SZn-Mito (0.5 μM) and (b) Mitotracker Red FM (1 μM) for 30 min at 37 °C. (c) Colocalized image. The wavelengths for TP and OP excitation were 760 and 514 nm, respectively, and the corresponding emissions were collected at 450−550 (SZn-Mito) and 600−700 nm (Mitotracker Red FM). Scale bar: 20 μm. Cells shown are representative images from replicate experiments (n = 5).

The dissociation constants (K_d^{OP} and K_d^{TP}) of SZn-Mito for the OP and TP processes were calculated from the fluorescence titration curves (Figure S3c).[16,18] The titration curves were fitted well with a 1:1 binding model (Figure S3c); the Hill plots were linear with a slope of 1.0 (Figure S3d), and the Job's plot exhibited a maximum point at a mole fraction of 0.50 (Figure S4), indicating 1:1 complexation between the probe and Zn^{2+}. The K_d^{OP} and K_d^{TP} values for Zn^{2+} were 3.1 nM; thus, this probe can detect Zn^{2+} in the nanomolar range.

SZn-Mito showed high selectivity for 1 μM Zn^{2+} over 1 mM Na^+, K^+, Ca^{2+}, and Mg^{2+} and 1 μM Mn^{2+}, Fe^{2+}, and Fe^{3+} but only modest selectivity over 1 μM Cd^{2+} (Figure S5b). In the presence of 1 μM Co^{2+}, Ni^{2+}, and Cu^{2+}, the fluorescence was quenched as a result of metal-to-ligand electron transfer upon excitation.[19] Since Co^{2+}, Ni^{2+}, and Cu^{2+} ions rarely exist in the cells,[20] this probe can detect $[Zn^{2+}]_m$ with minimum interference from other competing metal ions. Moreover, SZn-Mito is pH-insensitive in the biologically relevant pH range (Figure S5a).

The TP action spectra of SZn-Mito in MOPS buffer containing excess Zn^{2+} indicated a $\Phi\delta$ value of 75 GM at 750 nm (Figure 1b), which is comparable to those of existing TP probes.[12] This predicts a bright TPM image of the cells stained with SZn-Mito, as observed (Figure 2a). In comparison with Figure 2a, the TPM image of HeLa cells labeled with 0.5 μM RhodZin-3 AM was hardly visible and that labeled with 5 μM RhodZin-3 AM and 5 μM Pluronic F-127, a surfactant that enhances the cell loading,[8] was much dimmer (Figure S6). This result underlines the advantage of SZn-Mito over commercial probes in TPM imaging. Further, the TP-excited fluorescence (TPEF) spectrum of SZn-Mito in the cells was symmetrical and slightly blue-shifted relative to that measured in the MOPS buffer, with an emission maximum at 475 nm (Figure S7b), presumably because the polarity of the probe environment was

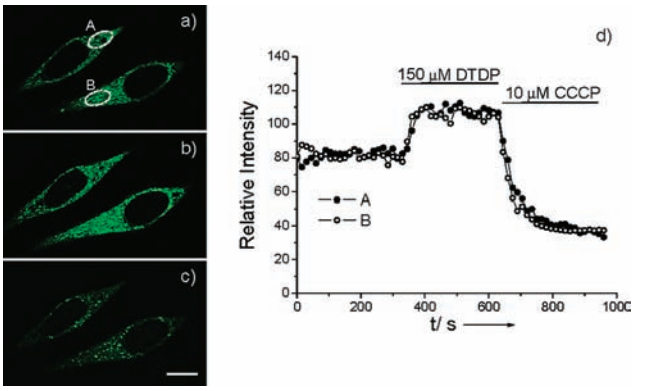

Figure 3. (a−c) TPM images of 0.5 μM SZn-Mito-labeled HeLa cells (a) before and (b) after addition of 150 μM DTDP to the imaging solution and (c) after addition of 10 μM CCCP to (b). (d) Relative TPEF intensity of SZn-Mito-labeled HeLa cells as a function of time. The TPEF intensities were collected at 425−575 nm upon excitation at 760 nm with femtosecond pulses. Scale bar: 10 μm. Cells shown are representative images from replicate experiments (n = 5).

rather homogeneous and slightly more hydrophobic than that of MOPS buffer. Therefore, we detected $[Zn^{2+}]_m$ by using the detection window at 425−575 nm.

To assess whether SZn-Mito can detect $[Zn^{2+}]_m$ in cells, the HeLa cells were colabeled with SZn-Mito and Mitotracker Red FM, a well-known OP probe for mitochondria.[8] The TPM and OPM images (Figure 2a,b) were obtained by using the detection windows at 450−550 and 600−700 nm, respectively, to selectively detect the two signals with equal intensities (Figure S8). The two images overlapped well (Figure 2c), and the Pearson's colocalization coefficient, A, for SZn-Mito and Mitotracker Red FM was 0.89, as calculated using Autoquant X2 software. In addition, the TPEF intensity of SZn-Mito-labeled HeLa cells decreased dramatically upon addition of *N*,*N*,*N*′,*N*′-tetrakis(2-pyridyl)ethylenediamine (TPEN), a membrane-permeable Zn^{2+} chelator that can effectively remove $[Zn^{2+}]_m$ (Figure S6c,d).[5b] These results confirmed that the bright regions in the TPM image reflect the presence of $[Zn^{2+}]_m$. Moreover, SZn-Mito showed negligible toxicity as measured by using a CCK-8 kit (Figure S9). Further, the TPEF intensity at a given spot on the SZn-Mito-labeled HeLa cells remained nearly the same after continuous irradiation with the femtosecond pulses for 60 min, indicating its high photostability (Figure S7d).

We then tested whether SZn-Mito could be used to monitor changes in $[Zn^{2+}]_m$ in live cells. The TPEF intensity increased when 2,2′-dithiodipyridine (DTDP; 150 μM), a reagent that promotes the release of Zn^{2+} from Zn^{2+}-binding proteins,[21] was added to HeLa cells labeled with SZn-Mito (Figure 3a,b), and it decreased upon addition of carbonyl cyanide *m*-chlorophenylhydrazone (CCCP; 10 μM), a compound that promotes the release of intramitochondrial cations by collapsing the mitochondrial membrane potential (Figure 3c).[10] Moreover, the TPEF intensity increased when the cells were treated with 100 μM Zn^{2+} and 100 μM pyrithione (2-mercaptopyridine *N*-oxide), a reagent that can bring Zn^{2+} into the cytoplasm,[22] and decreased upon treatment with CCCP (Figure S10). These results established the capability of SZn-Mito for detecting $[Zn^{2+}]_m$ in live cells for a long period of time with minimum interference from other competing metal ions, pH, cytotoxicity, and photostability.

We further investigated the utility of this probe in tissue imaging. TPM images were obtained from a slice of 14-day-old

dx.doi.org/10.1021/ja200444t |*J. Am. Chem. Soc.* 2011, 133, 5698–5700

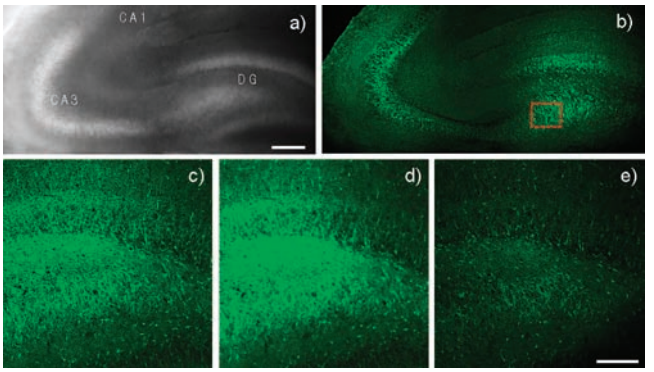

Figure 4. Images of a rat hippocampal slice stained with 20 μM SZn-Mito for 1 h. (a) Bright-field images of the CA1 and CA3 regions and the dentate gyrus (DG) at 10× magnification. (b) 10 TPM images along the z direction at depths of 100−200 μm were accumulated. (c−e) Magnification at 40× in the DG region [red box in (b)] at a depth of ∼100 μm (c) before and (d) after addition of 150 μM DTDP to the imaging solution and (e) after addition of 10 μM CCCP to (d). Scale bars: (a) 300 and (e) 75 μm.

rat hippocampal tissue incubated with 20 μM SZn-Mito for 1 h at 37 °C. The slice from the brain was too large to show with one image, so two images were obtained in each plane and combined. The bright-field image (Figure 4a) revealed the CA1 and CA3 regions and also the dentate gyrus (DG). As the structure of the brain tissue is known to be inhomogeneous in its entire depth, we accumulated 10 TPM images at depths of 100−200 μm to visualize the distributions of $[Zn^{2+}]_m$ (Figure 4b). They revealed intense fluorescence in the CA3 and DG regions (Figure 4a).[23] The increase in the TPEF intensity after addition of DTDP and the decrease upon treatment of CCCP provide strong evidence that the bright regions reflect the presence of $[Zn^{2+}]_m$ (Figure 4d,e). At a higher magnification, the $[Zn^{2+}]_m$ distribution in the DG region was clearly visualized (Figure 4c). Moreover, the TPM images obtained at a depth of 100−200 μm revealed the $[Zn^{2+}]_m$ distribution in the given plane along the z direction in the DG region (Figure S11). Hence, SZn-Mito is clearly capable of detecting $[Zn^{2+}]_m$ at a depth of 100−200 μm in living tissues through TPM. Further, the TPM images shown in Figure 4b−d are much brighter than those stained with 40 μM RhodZin-3 AM and 80 μM Pluronic F-127 for 1.5 h, demonstrating the advantage of SZn-Mito over RhodZin-3 AM (Figure S11).

In conclusion, we have developed a TP probe (SZn-Mito) that shows a 7-fold TPEF enhancement in response to Zn^{2+}, a maximum TP action cross section of 75 GM in the presence of excess Zn^{2+}, a dissociation constant (K_d^{TP}) of 3.1 ± 0.1 nM, and pH insensitivity in the biologically relevant range. Better than the currently available probes, this novel probe can selectively detect $[Zn^{2+}]_m$ in living tissues at a depth of 100−200 μm without interference from other metal ions.

■ ASSOCIATED CONTENT

Supporting Information. Synthesis and photophysical properties of SZn-Mito, cell culture, and two-photon imaging. This material is available free of charge via the Internet at http://pubs.acs.org.

■ AUTHOR INFORMATION

Corresponding Author
kimhm@ajou.ac.kr; chobr@korea.ac.kr

■ ACKNOWLEDGMENT

This work was supported by the National Research Foundation (NRF) through grants funded by the Korean Government (2010-0016997 and 2010-0018921), the Priority Research Centers Program through the NRF funded by the Ministry of Education, Science, and Technology (2010-0028294 and 2010-0020209), and the Ajou University Research Fellowship of 2010. C.S.L., H.J.K., and J.H.H. were supported by BK21 Scholarships.

■ REFERENCES

(1) Frederickson, C. J. *Int. Rev. Neurobiol.* **1989**, *31*, 145.
(2) (a) Weiss, J. H.; Sensi, S. L.; Koh, J. Y. *Trends Pharmacol. Sci.* **2000**, *21*, 395. (b) Bitanihirwe, B. K.; Cunningham, M. G. *Synapse* **2009**, *63*, 1029.
(3) Nakashima, A. S.; Dyck, R. H. *Brain Res. Rev.* **2009**, *59*, 347.
(4) (a) Bush, A. I. *Curr. Opin. Chem. Biol.* **2000**, *4*, 184. (b) Bush, A. I. *Trends Neurosci.* **2003**, *26*, 207. (c) Barnham, K. J.; Bush, A. I. *Curr. Opin. Chem. Biol.* **2008**, *12*, 222.
(5) (a) Sensi, S. L.; Yin, H. Z.; Weiss, J. H. *Eur. J. Neurosci.* **2000**, *12*, 3813. (b) Sensi, S. L.; Ton-That, D.; Sullivan, P. G.; Jonas, E. A.; Gee, K. R.; Kaczmarek, L. K.; Weiss, J. H. *Proc. Natl. Acad. Sci. U.S.A.* **2003**, *100*, 6157.
(6) Sensi, S. L.; Paoletti, P.; Bush, A. I.; Sekler, I. *Nat. Rev. Neurosci.* **2009**, *10*, 780.
(7) Sensi, S. L.; Ton-That, D.; Weiss, J. H.; Rothe, A.; Gee, K. R. *Cell Calcium* **2003**, *34*, 281.
(8) *A Guide to Fluorescent Probes and Labeling Technologies*, 10th ed.; Haugland, R. P., Ed.; Molecular Probes: Eugene, OR, 2005.
(9) (a) Tomat, E.; Nolan, E. M.; Jaworski, J.; Lippard, S. J. *J. Am. Chem. Soc.* **2008**, *130*, 15776. (b) Dittmer, P. J.; Miranda, J. G.; Gorski, J. A.; Palmer, A. E. *J. Biol. Chem.* **2009**, *284*, 16289.
(10) Caporale, T.; Ciavardelli, D.; Di Ilio, C.; Lanuti, P.; Drago, D.; Sensi, S. L. *Exp. Neurol.* **2009**, *218*, 228.
(11) (a) Helmchen, F.; Denk, W. *Nat. Methods* **2005**, *2*, 932. (b) Zipfel, W. R.; Williams, R. M.; Webb, W. W. *Nat. Biotechnol.* **2003**, *2*, 1369.
(12) (a) Kim, H. M.; Cho, B. R. *Acc. Chem. Res.* **2009**, *42*, 863. (b) Kim, H. M.; Cho, B. R. *Chem.—Asian J.* **2011**, *6*, 58.
(13) (a) Nolan, E. M.; Lippard, S. J. *Acc. Chem. Res.* **2009**, *42*, 193. (b) Que, E. L.; Domaille, D. W.; Chang, C. J. *Chem. Rev.* **2008**, *108*, 1517. (c) Komatsu, K.; Kikuchi, K.; Kojima, H.; Urano, Y.; Nagano, T. *J. Am. Chem. Soc.* **2005**, *127*, 10197.
(14) (a) Murphy, M. P.; Smith, R. A. *Annu. Rev. Pharmacol. Toxicol.* **2007**, *47*, 629. (b) Yousif, L. F.; Stewart, K. M.; Kelley, S. O. *ChemBioChem* **2009**, *10*, 1939.
(15) (a) Dickinson, B. C.; Srikun, D.; Chang, C. J. *Curr. Opin. Chem. Biol.* **2010**, *14*, 50. (b) Dickinson, B. C.; Chang, C. J. *J. Am. Chem. Soc.* **2008**, *130*, 9638.
(16) Kim, H. J.; Han, J. H.; Kim, M. K.; Lim, C. S.; Kim, H. M.; Cho, B. R. *Angew. Chem., Int. Ed.* **2010**, *49*, 6786.
(17) Kim, H. M.; Choo, H. J.; Jung, S. Y.; Ko, Y. G.; Park, W. H.; Jeon, S. J.; Kim, C. H.; Joo, T.; Cho, B. R. *ChemBioChem* **2007**, *8*, 553.
(18) Kim, M. K.; Lim, C. S.; Hong, J. T.; Han, J. H.; Jang, H. Y.; Kim, H. M.; Cho, B. R. *Angew. Chem., Int. Ed.* **2010**, *49*, 364.
(19) Akkaya, E. U.; Huston, M. E.; Czarnik, A. W. *J. Am. Chem. Soc.* **1990**, *112*, 3590.
(20) Rae, T. D.; Schmidt, P. J.; Pufahl, R. A.; Culotta, V. C.; O'Halloran, T. V. *Science* **1999**, *284*, 805.
(21) Aizenman, E.; Stout, A. K.; Hartnett, K. A.; Dineley, K. E.; McLaughlin, B.; Reynolds, I. J. *J. Neurochem.* **2000**, *75*, 1878.
(22) (a) Barnett, B. L.; Kretschmar, H. C.; Hartman, F. A. *Inorg. Chem.* **1977**, *16*, 1834. (b) Chandler, C. J.; Segel, I. H. *Antimicrob. Agents Chemother.* **1978**, *14*, 60.
(23) Kim, H. M.; Seo, M. S.; An, M. J.; Hong, J. H.; Tian, Y. S.; Choi, J. H.; Kwon, O.; Lee, K. J.; Cho, B. R. *Angew. Chem., Int. Ed.* **2008**, *47*, 5167.